View Article Online / Journal Homepage / Table of Contents for this issue
Dynamic Article Links

Journal of
Materials Chemistry

Cite this: *J. Mater. Chem.*, 2012, **22**, 25065

www.rsc.org/materials

PAPER

Thermal and photoinduced liquid crystalline phase transitions with a rod–disc alternative change in the molecular shape†

Daisuke Tanaka,[ab] Hisato Ishiguro,[ab] Yo Shimizu*[b] and Kingo Uchida*[a]

Received 15th August 2012, Accepted 1st October 2012
DOI: 10.1039/c2jm35518c

A triphenylene derivative which has six 4-tetradecyloxyazobenzene units connected with propylene–ester linkages (**1**) was synthesised to study the liquid crystalline phase transitions in both thermotropic and photo-induced manners. It was found that **1** exhibits smectic A (SmA) and rectangular columnar ($\mathrm{Col_r}$) mesophases in an enantiotropic way. This means that **1** can behave as both rod- and disc-like molecules depending on the thermal condition. To the best of our knowledge, this is the first case in thermotropic liquid crystals where one compound exhibits both calamitic and discotic mesomorphism with the change of molecular shape in anisotropy. Under the photo-irradiation at 365 nm of wavelength which induces a photoisomerisation of azobenzene units from *trans* to *cis* forms, the phase transitions take place in the same manner as in the thermotropic ones with a certain decrease of phase transition temperatures. It is also a new finding that at 202.5 °C at which **1** exhibits a $\mathrm{Col_r}$ mesophase without photo-irradiation, the successive phase changes are induced by increasing the light intensity to the isotropic liquid (Iso) phase by way of a SmA phase. This means that the isothermal phase transitions among Iso, SmA and $\mathrm{Col_r}$ phases can be controlled by light intensity. This is also the first example that the isothermal liquid crystalline phase transitions are controlled by photo-irradiation among three phases ($\mathrm{Col_r}$, SmA and Iso), which are also accompanied with the shape change of molecules between rod and disc.

Introduction

Liquid crystals (LCs) can be categorised into two types, calamitic and discotic LCs, based on different molecular shapes in anisotropy.[1] A rod-like anisotropy of the molecule for the former and a disc-like one for the latter exhibit their own characteristic mesomorphism. The molecular anisotropy is expressed by the ratio of the longitudinal and lateral lengths of a molecule. Therefore, the characteristic liquid crystalline phases of calamitic and discotic LCs are smectic and columnar phases, respectively. The former has layered orders of molecules and the latter a molecularly stacking order to form a column which makes arrays in a 2-dimensional way. However, recent studies on liquid crystalline phase transitions of supramolecular systems have shown a variety of mesomorphisms and molecules that are not rod-like or disc-like sometimes show mesomorphism by way of formation of molecular assemblies with intermolecular interactions, of which shapes are anisotropic such as rod-like and disc-like.[2] Furthermore, one can see a series of compounds such as dendrimer LCs which sometimes exhibit a bimesomorphism (calamitic and discotic LC phases) depending on the generation and chain length.[3] However, no mesogen has been found to exhibit a bimesomorphism accompanied by the shape change of molecules between rod and disc.

Previously, we synthesised a triphenylene derivative with six peripherally attached 4-decyloxyazobenzene units (**1-C10**) connected by propylene-carbonyloxy groups to a triphenylene core (Fig. 1) to reveal the mesomorphism and it was found that **1-C10** exhibits a hexagonal columnar ($\mathrm{Col_h}$) mesophase as a monotropic phase. However, upon relatively rapid cooling from the isotropic liquid (Iso) phase (*ca.* 5 °C $\mathrm{min^{-1}}$), a smectic A (SmA) phase is formed as a transient liquid crystalline phase as a monotropic one. This SmA phase spontaneously transitions to the $\mathrm{Col_h}$ phase under isothermal conditions, meaning that the SmA phase is thermodynamically metastable (Fig. S1 in the ESI†).[4] One year before our report, the liquid crystalline properties of the similar triphenylene–azobenzene systems with different linkage groups have been studied by Rahman *et al.* to show that those derivatives show only discotic columnar mesomorphism upon both heating and cooling.[5] These results indicate that the bimesomorphism shown by **1-C10** is profoundly related to the flexibility/rigidity of the linkage group between a

---

[a] *Department of Materials Chemistry, Faculty of Science and Technology, Ryukoku University, Seta, Otsu, Shiga 520-2194, Japan. E-mail: uchida@rins.ryukoku.ac.jp; Fax: +81 77 543 7483; Tel: +81 77 543 7462*
[b] *Synthetic Nano-Function Materials Group, Research Institute for Ubiquitous Energy Devices, National Institute of Advanced Industrial Science and Technology (AIST), Kansai Centre, Midorigaoka, Ikeda, Osaka 563-8577, Japan. E-mail: yo-shimizu@aist.go.jp; Fax: +81-72-751-9525; Tel: +81-72-751-9628*

† Electronic supplementary information (ESI) available: Optical textures, XRD, and transient absorption spectra of **1-C14**. See DOI: 10.1039/c2jm35518c

triphenylene core and azobenzene units and therefore, the packing mode should be considered for the interpretation of mechanism, in which the motion of alkoxyazobenzenes is hindered to some extent by the linkage groups. This leads to a molecular design, change of alkyl length, to obtain such a unique phase transition with the change of molecular shape in an enantiotropic way.

On the other hand, control of the molecular alignment and orientational order of LCs has also been performed by the action of light.[6,7] In particular, azobenzene has been extensively applied as a photo-switchable trigger dopant for phase transitions. Such photo-induced phase transitions, however, are limited to the transitions between the relatively lower ordered calamitic LC phases such as nematic (N) and SmA phases and all results in these photo-induced phase transitions are of disordering to the Iso phase, except for one case where the photo-induced phase transitions between smectic C (SmC) and a bicontinuous cubic mesophase, though the molecular anisotropy is not changed between rod and disc.[8] To the best of our knowledge, the photo-interconversion between different categories of LC systems, *i.e.* calamitics and discotics, has not been reported so far.

In this paper, we report a unique mesomorphism for both thermal and photo-induced phase transitions of one mesogen, **1-C14**, that consists of a discotic central core of triphenylene and six rod-like azobenzene units with terminal tetradecyloxy chains which are covalently connected by propylene-carbonyloxy groups. It was found that **1-C14** exhibits both calamitic SmA and discotic Col$_r$ phases in both thermotropic and photo-induced isothermal manners that are accompanied with the change of molecular anisotropy in shape between rod and disc. The concept is schematically shown in Fig. 1.

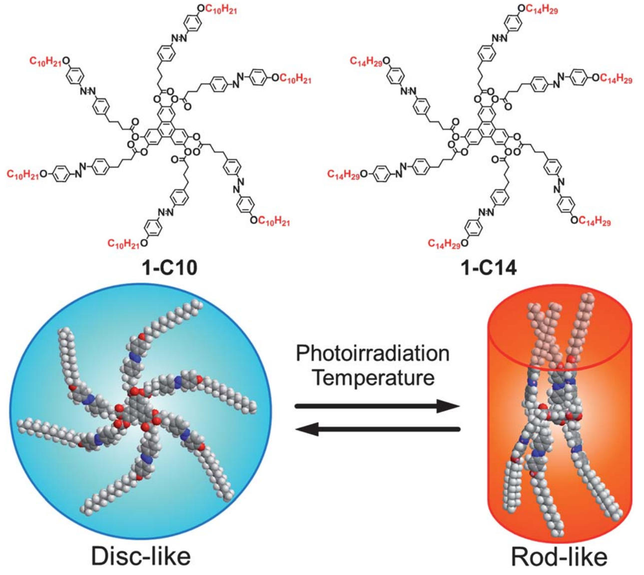

Fig. 1 Chemical structures and reversible molecular shape changes of **1-C10** and **1-C14**. Schematic illustration of LC molecules which could behave as rod-like (calamitic) and disc-like (discotic) liquid crystals, suggesting a "smart molecule" against external stimuli such as temperature and photo-irradiation. The compound **1-C14** was studied in this work.

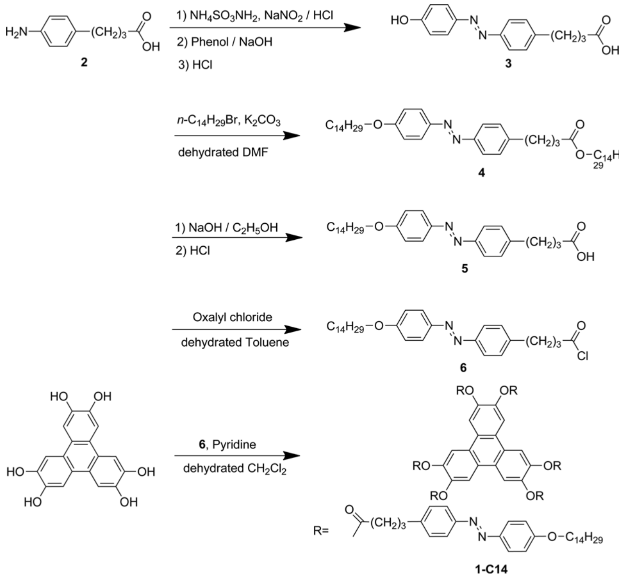

Scheme 1 Synthetic routes towards a tetradecyloxy homologue of the triphenylene mesogen.

Results and discussion

The synthesis of triphenylene-2,3,6,7,10,11-hexayl hexakis[4-(4-{[4-(tetradecyloxy)phenyl]diazenyl}phenyl)butanoate] (**1-C14**) was carried out by a route shown in Scheme 1. The method was also applied for the synthesis of **1-C10**.[4] The azobenzene derivative 4-{4-[(4-hydroxyphenyl)diazenyl]phenyl}butanoic acid (**3**) was initially prepared followed by esterification and ether formation of both ends of the molecule with 1-bromotetradecane by the Williamson method. Hydrolysis of the ester moiety of the formed tetradecyl-4-(4-{[4-(tetradecyloxy)phenyl]diazenyl}phenyl) butanoate (**4**) was carried out in NaOH ethanol solution to form 4-(4-{[4-(tetradecyloxy)phenyl]diazenyl}phenyl)butanoic acid (**5**).

The acid **5** was converted to acid chloride (**6**) and it was reacted with 2,3,6,7,10,11-hexahydroxytriphenylene to form **1-C14**. The obtained **1-C14** was purified by silica gel chromatography (chloroform anhydrous) followed by recrystallization from chloroform anhydrous.

LC characterisation was performed by optical texture observations under cross-polarised conditions using a polarised optical microscope equipped with a temperature-controllable hot stage, as well as by differential scanning calorimetry (DSC) and X-ray diffraction (XRD) measurements. Optical images were monitored for the samples between two glass substrates coated with polyimide film to obtain homogeneous alignment (parallel to the substrate plane). The DSC measurements indicated that two enantiotropic LC phases were formed as shown in Fig. 2a. Two broad endothermic peaks are seen in the heating run at 160–185 °C and *ca.* 205 °C, in addition to a sharp peak at 206 °C. For the cooling run, four sharp exothermic peaks arise at 207 °C, 203 °C, 126 °C and 117 °C. The optical textures observed at 209.8 °C are shown in Fig. 2b in which the "bâtonnets" texture is growing. "Bâtonnets" is a well-known texture that arises at the early stage of calamitic SmA domain formation, and it is typically seen in the nucleation of SmA phase domains.[1] These "bâtonnets" grow into a fan texture upon further cooling (Fig. 2c

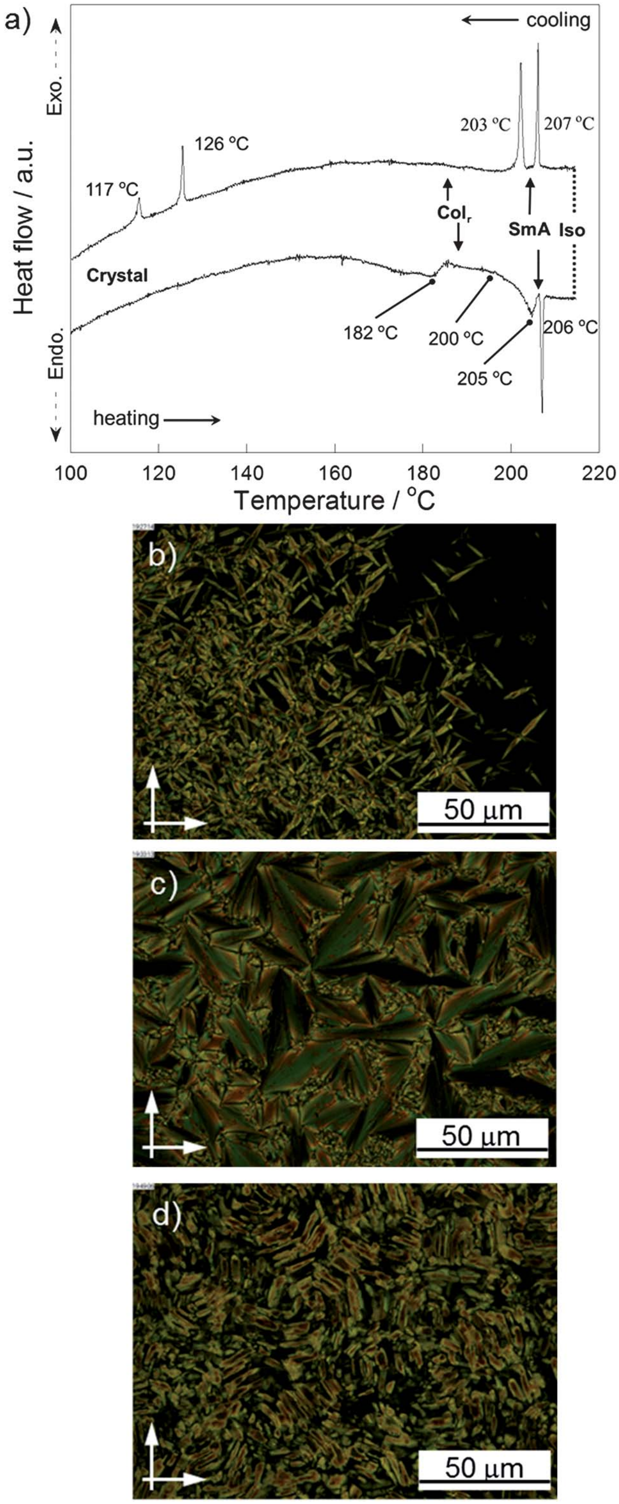

Fig. 2 DSC curve and the optical images of each phase: (a) DSC traces of **1-C14** at heating and cooling rates of 1 °C min^{-1}. The optical texture changes at the phase transitions during the cooling process, (b) the "bâtonnets" texture arises at 209.8 °C, (c) the fan-shaped texture is formed by the growth of "bâtonnets" and (d) the optical texture changes at 203.1 °C corresponding to the SmA-to-Col$_r$ transition on cooling. The arrows in the images indicate the polarising direction of the analyser and polariser.

and Fig. S2c in the ESI†) and finally change into a texture of the Col$_r$ phase at 203.1 °C as shown in Fig. 2d.

By monitoring the phase transition with an optical microscope, the start of the phase transition was observed around 210 °C which is the clearing point from SmA to Iso phases, as evidenced by the formation of "bâtonnets" in the isotropic dark image under the cross-polarisation conditions (Fig. 2b and Fig. S2a and b in the ESI†) with glass substrates coated with polyimide.

Formation of a dark image was observed for the sandwiched film between bare glass substrates with a polarised microscope under the cross-polarisation conditions, indicating that the molecules strongly tend to align in a homeotropic way (perpendicular orientation to the substrate plane) between bare glass substrates, although the "bâtonnets" emerge at the early stage of the Iso–SmA phase transition and then spontaneously change to a dark image (Fig. S2d in the ESI†). The enthalpy change of the Iso–SmA phase transition is 8 kJ mol^{-1}, which is much higher than that of typical SmA–Iso transitions ($\leq$1 kJ mol^{-1}): this would appear reasonable, considering that six azobenzene units are contained in each molecule. Further cooling of the sample leads to a change in optical texture from a fan-like to a columnar-like one (Fig. 2d and Fig. S2e and f in the ESI†).

The XRD measurements of the non-aligned sample gave a pattern that is assigned to a Col$_r$ phase (Fig. S3 in the ESI†) with symmetry *P*2/*a* (lattice constants: a = 92.9 Å, b = 59.6 Å, see Table S1 in the ESI†). A small and broad peak corresponding to the stacking periodicity of a columnar structure (*ca.* 3.5 Å) is seen, indicating disordering of the molecular stacking.

The XRD pattern of the SmA phase was also detected as a typical one for layered structures (Fig. S4 and Table S2 in the ESI†) with a simple sequence of reflections for the layer spacing ($d_{100} : d_{200} : d_{300} = 1 : 1/2 : 1/3$). The observed layer spacing (53.1 Å) is shorter than twice that of the azobenzene mesogenic unit (32.7 Å), probably due to the interdigitating alkyl chains. Therefore, two possibilities of molecular arrangement for the SmA layer should be considered: monolayer and bilayer. Based on the molecular models of mesogenic azobenzene and triphenylene core, it is difficult to position the six azobenzene units at one side of the triphenylene plane to produce a face-to-face orientation of the two triphenylene units, which would form a bilayer structure (Fig. S5 in the ESI†). Therefore, the SmA layer should be a monolayer in which one molecule typically has three azobenzene units on each side of the triphenylene plane. Interestingly, an excimer emission corresponding to its dimeric triphenylenes could not be detected in either the SmA or Col$_r$ phase of the film.[9]

Therefore, it is concluded that **1-C14** exhibits two enantiotropic LC phases, SmA and Col$_r$ (*P*2/*a*) phases, and thus that the molecules change their shapes between rod-like and disc-like anisotropies at the phase transition, considering the molecular length and diameter of rod- and disc-like conformations of **1-C14** (Fig. S6 in the ESI†). The azobenzene moieties bundle to form a rod-shaped molecule in the former, and the latter gives an image of azobenzene moieties forming a disc-shaped molecule in which the azobenzene moieties change directions to share the plane of the triphenylene core, just as a flower blooms. Compared with **1-C10**, **1-C14** has longer alkyl terminal chains with only 4 carbons and an increased rod-shaped side area (Fig. 1), which enhances the van der Waals forces between the rod-shaped molecules positioned side by side (Fig. S7 in the ESI†). Then, the SmA phase of **1-C14** was stabilised. As can be seen in the LC system, the phase transitions are governed by a fine balance between van der Waals interaction energies among the molecules and the total energy of the system.

On the other hand, it was found that **1-C14** clearly exhibits phase transitions under UV light irradiation ($\lambda = 365$ nm, 1.0 W cm^{-2}) in the same manner as observed without UV light irradiation (Fig. 3). The observed phase transition temperatures under UV irradiation decreased by *ca.* 9 °C and *ca.* 7 °C for the Iso-to-SmA and SmA-to-Col$_r$ transitions, respectively.

These decreases in the phase transition temperatures are due to the *trans–cis* photoisomerisation of the azobenzene units in **1-C14**, implying that the shape change of the azobenzene moiety from a linear rod to a bent rod destabilises the LC phases.[10] The photo-induced isomerisation of azobenzene units is still active in a toluene solution, although they are densely connected to a triphenylene core (Fig. S8 in the ESI†).[11] The activation energy of thermal *cis* to *trans* isomerisation of the azobenzene moieties of **1-C14** in the toluene solution was obtained to be 91.8 kJ mol^{-1} (Fig. S9 in the ESI†), and formation of *cis*-azobenzene has hardly been considered at an elevated temperature such as 200 °C. However, generation of the absorption band of the *cis*-form of **1-C14** azobenzene moieties in a liquid crystalline state at 200 °C was detected within a time of 50 ns by flash photolysis using a nanosecond-scale 355 nm laser pulse (Quanta-Ray THG, DCR-3 Nd^{3+}:YAG laser, with an intensity of 3–5 mJ per pulse: Fig. S10 and S11 in the ESI†). This detection was made by monitoring the absorbance of the LCs using the transmitted light. The band disappeared after 100 μs of pulsed light irradiation.

Additionally, in order to confirm that the temperature of the LC was not enhanced under UV irradiation ($\lambda = 365$ nm, 1.0 W cm^{-2}) at 200 °C, the open LC surface was monitored under irradiation with a thermographic camera. It was found that the temperature rise was only 1 °C at the film surface (Fig. S12 and S13 in the ESI†). The above results indicate that the phase transition takes place in an equilibrium manner and the *trans–cis* photoisomerisation effectively competes with the *cis–trans* back reaction as the thermal isomerisation occurring at high temperature.[12]

On the other hand, Yagai and his co-workers reported the synthesis and photoresponse of disc-shaped aggregates (each consisting of six triangle parts to form a single rosette styled aggregate) having six azobenzene moieties, with the photo-isomerisation of one of them drastically destabilising the stacking interaction between rosettes.[13] This information supports the notion that isomerisation of a small amount of the azobenzene moieties is adequate to induce the phase changes in our system. Upon UV irradiation of **1-C14** in the smectic LC phase, one of the azobenzene moieties bent and destabilised the phase, thus inducing the phase transitions. With decreasing light intensity, the portion of **1-C14** molecules having only one *cis*-azobenzene moiety decreases and a phase change proceeded to thermally

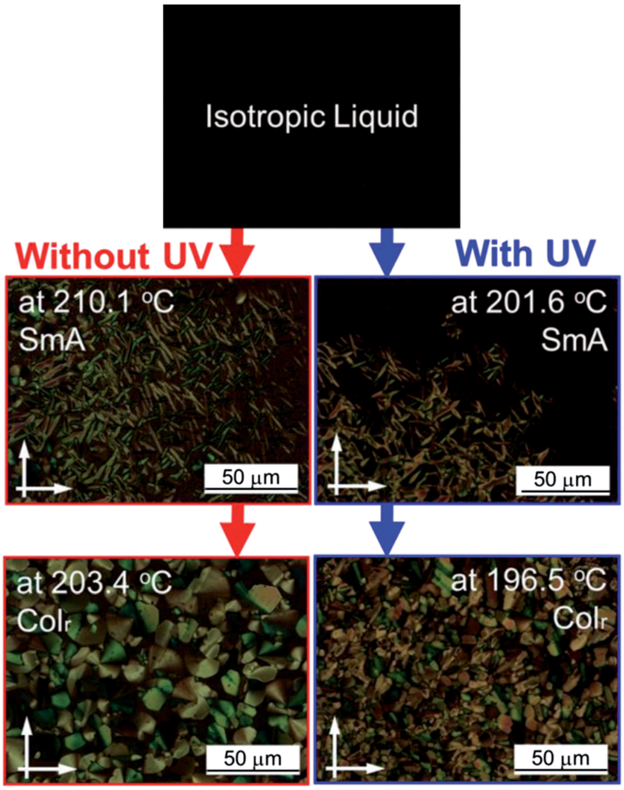

Fig. 3 Phase transitions during the cooling process with and without UV light irradiation: for non-irradiation (left side) and for UV light irradiation at 365 nm (right side). The observed temperatures corresponding to the phase transitions of Iso–SmA and SmA–Col$_r$ decreased by 7–9 °C under the UV light irradiation. The arrows indicate the polarising directions of the analyser and polariser.

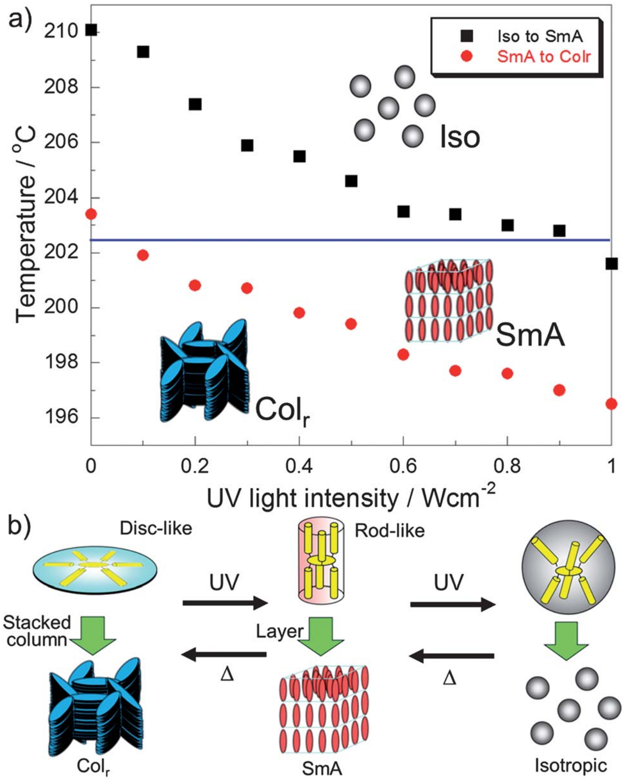

Fig. 4 Isothermal molecular shape and LC phase changes depending on UV light intensity: (a) schematic illustration of isothermal phase transitions, (b) phase diagram showing irradiated UV light intensity (blue line at around 202.5 °C corresponds to a pathway for controlling photoinduced phase transitions among the Col$_r$, SmA and Iso phases).

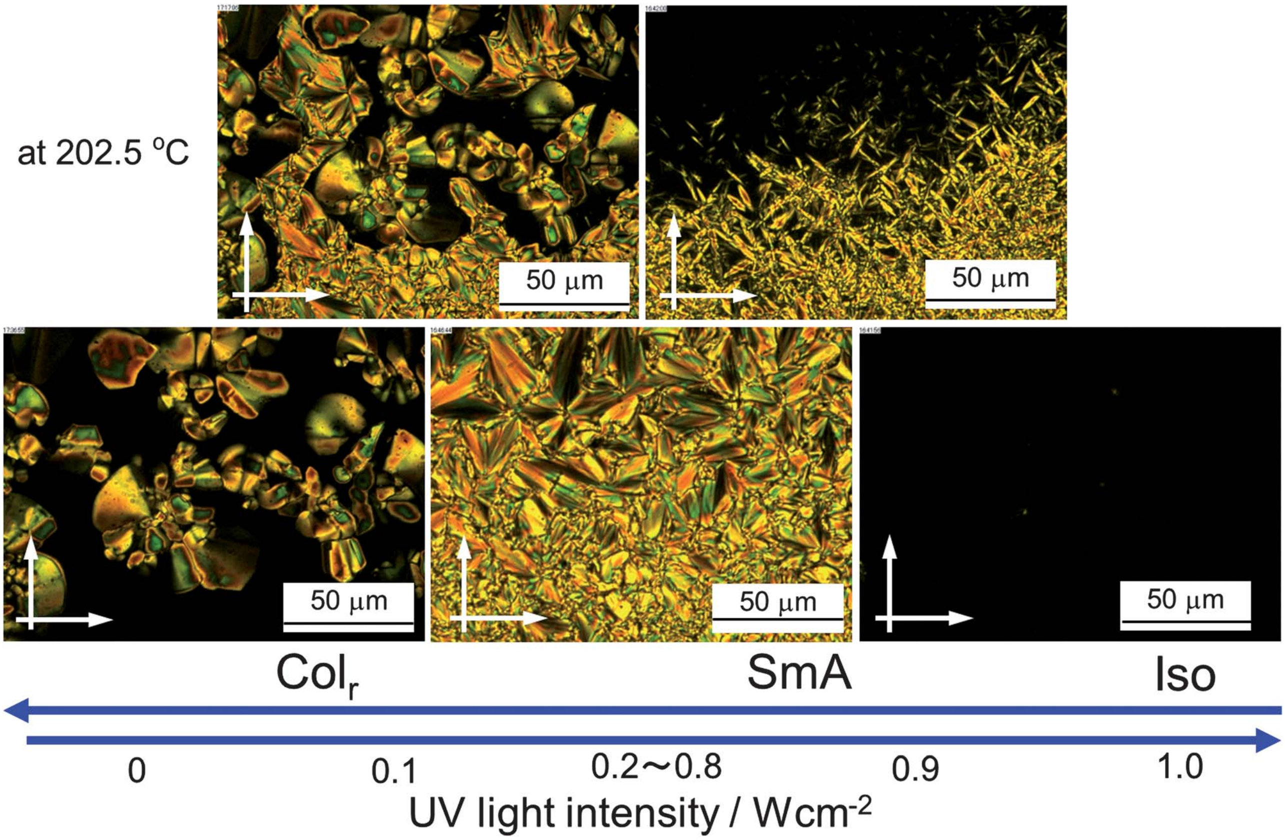

Fig. 5 Textures of **1-C14** during isothermal phase transitions depending on the light intensity of 365 nm.

stable discotic phases. By increasing the light intensity, the percentage of **1-C14** molecules having one *cis*-azobenzene moiety increases. Even in this period, equilibrium is achieved between thermal recovery of *trans*-azobenzene and photo-induced *cis*-azobenzene formation. By increasing the UV light intensity, the population of **1-C14** molecules having one *cis*-azobenzene moiety is further increased, and finally even the stable discotic LC phase is destroyed to form the Iso phase. The XRD measurements revealed that the identified LC phases formed even under UV irradiation (Fig. S14, Tables S3 and S4 in the ESI†). Additionally, a phase transition diagram upon cooling under constant light intensity is shown in Fig. 4b. The phase transition temperatures of the Iso-to-SmA and SmA-to-Col$_r$ transitions decrease as the UV light intensity increases. In particular, it is interesting to note that an isothermal line can be drawn for the entire UV light intensity range at *ca.* 202.5 °C, strongly indicating that under varying UV light intensity the isothermal phase transitions can take place among the Col$_r$, SmA and Iso phases. In other words, it is possible to control the phase transitions among the three phases by tuning the light intensity. In fact, we can see that reversible phase transitions are produced solely by the light intensity change (Fig. 5).

Conclusions

It was found that **1-C14** exhibits a phase transition sequence of crystal–Col$_r$–SmA–Iso phases in both thermotropic and photo-induced isothermal ways. These unique LC phase transitions should be accompanied with the change of molecular shape in anisotropy between rod and disc. To the best of our knowledge, **1-C14** is the first compound exhibiting such unique LC phase transitions and this is from the nature of ordered fluid as soft matter. In addition, it is so interesting to find that the same LC phase transitions can be controlled by the light intensity of UV irradiation under isothermal conditions. This means that every anisotropic functional property arises under control of temperature and light intensity. For example, this characteristic phase transition is expected to show a new function based on the change of anisotropic properties such as charge transport and light transmittance. In particular, it is important to see electronic properties, considering that recent studies on charge transport in liquid crystalline media have shown a high carrier mobility of charges in highly ordered mesophases which reaches the mobility of amorphous Si ($\sim 10^{-1}$ cm^2 V^{-1} s^{-1}).[14] Furthermore, these findings might provide a building block toward developing a new type of molecular machine for non-contact and remote-controlled devices that can be driven by photon flux as well as thermal conditions in relation to new applications for robots made of soft materials.[15]

Further studies should be carried out to clarify the mechanism of these phase transitions and find out how a small number of *cis*-azobenzene moieties induce the phase changes.

Experimental

Materials

NMR spectra were obtained on a Bruker AVANCE 400 (400 MHz) spectrometer using deuterated solvents as the lock.

The spectra were collected at 25 °C and chemical shifts (δ, ppm) were referenced to the residual solvent peak (1H, $CDCl_3$ at 7.26 ppm). In the assignments, the chemical shift (in ppm) is given first, followed, in brackets, by multiplicity (s, singlet; d, doublet; t, triplet; m, multiplet; br, broad), the value of the coupling constants in Hz if applicable, the number of protons implied and finally the assignment.

Synthesis

4-{4-[(4-Hydroxyphenyl)diazenyl]phenyl}butanoic acid (3). To a reaction flask containing 200 mL of 0.1 M HCl and kept at 5 °C on an ice bath, 1.25 g (7.00 mmol) of 4-(4-aminophenyl)butanoic acid (**2**) and 0.48 g (7.00 mmol) of $NaNO_2$ were added, successively. After the compounds were dissolved by stirring at the temperature, 0.80 g (7.00 mmol) of $NH_4SO_3NH_2$ was added followed by addition of phenol 0.72 g (7.8 mmol) in 0.1 M NaOH 320 mL, and stirred at 5 °C for 20 min. Then the solution was acidified (pH: 3) by the addition of 2 M HCl. Precipitated crystals were filtered off and washed with water. The crystals were dried under vacuum to obtain 1.72 g (6.05 mmol) of **3** as a brown powder in 86.7% yield. **3**: m.p. 164.9–166.5 °C ^1H NMR (400 MHz, $CDCl_3$) $\delta = 1.25$ (br, H, $PhO\mathit{H}$), 2.01 (tt, $J = 7.6$, 7.4 Hz, 2H, $PhCH_2\mathit{CH_2}$), 2.40 (t, $J = 7.4$ Hz, 2H, $Ph\mathit{CH_2}$), 2.75 (t, $J = 7.6$ Hz, 2H, $PhCH_2CH_2\mathit{CH_2}$), 6.94 (d, $J = 8.9$ Hz, 2H, 2, 6-H Ar), 7.31 (d, $J = 8.5$ Hz, 2H, 3′, 5′-H Ar), 7.80 (d, $J = 8.5$ Hz, 2H, 2′, 6′-H Ar), 7.86 ppm (d, $J = 8.9$ Hz, 2H, 3, 5-H Ar).

Tetradecyl-4-(4-{[4-(tetradecyloxy)phenyl]diazenyl}phenyl) butanoate (4). K_2CO_3 4.91 g (35.2 mmol) and 1-bromotetradecane 2.09 mL (7.04 mmol) were added to 120 mL of dimethylformamide (DMF) anhydrous solution containing 1.00 g (3.52 mmol) of **3** under argon atmosphere, successively. The mixture was heated at 80 °C for 3 h. After cooling to room temperature, 100 mL of ether and 100 mL of water were added, then the separated water layer was extracted twice with 100 mL of ether. The organic layers were combined and washed with water (100 mL × 3). The combined organic layer was dried over sodium sulfate anhydrous, and the solvents were evaporated *in vacuo*. The crude product was purified by silica gel chromatography to obtain 1.68 g (2.48 mmol) of **4** in 70.1% yield. M.p. 118.4–119.4 °C; ^1H NMR (400 MHz, $CDCl_3$) $\delta = 0.87$ (t, $J = 6.9$ Hz, 3H, $COO(CH_2)_{13}\mathit{CH_3}$), 0.88 (t, $J = 6.9$ Hz, 3H, $PhO(CH_2)_{13}\mathit{CH_3}$), 1.18–1.67 (m, 46H, $PhOCH_2CH_2(\mathit{CH_2})_{11}$, $COOCH_2(\mathit{CH_2})_{12}$), 1.82 (tt, $J = 6.9$, 6.0 Hz, 2H, $PhOCH_2\mathit{CH_2}$), 2.00 (tt, $J = 7.5$, 7.4 Hz, 2H, $PhCH_2\mathit{CH_2}$), 2.34 (t, $J = 7.4$ Hz, 2H, $Ph\mathit{CH_2}$), 2.72 (t, $J = 7.5$ Hz, 2H, $PhCH_2CH_2\mathit{CH_2}$), 4.04 (t, $J = 6.0$ Hz, 2H, $PhO\mathit{CH_2}$), 4.07 (t, $J = 6.2$ Hz, 2H, $COO\mathit{CH_2}$), 6.99 (d, $J = 9.0$ Hz, 2H, 2, 6-H Ar), 7.30 (d, $J = 8.4$ Hz, 2H, 3′, 5′-H Ar), 7.80 (d, $J = 8.4$ Hz, 2H, 2′, 6′-H Ar), 7.89 ppm (d, $J = 9.0$ Hz, 2H, 3, 5-H Ar).

4-(4-{[4-(Tetradecyloxy)phenyl]diazenyl}phenyl)butanoic acid (5). Compound **4** (0.50 g, 0.74 mmol) was added into 210 mL of ethanol, and it was heated to 55 °C and stirred, until the mixture turned into a solution. Then, 18 mL of 10 wt% NaOH and 18 mL of water were added to the solution, and stirred for 1.5 h at the same temperature. After the reaction mixture was cooled down to ambient temperature, 40 mL of ethyl acetate, 10 mL of hexane, and 50 mL of water were poured into the mixture. The separated water layer was acidified to pH 3 by the addition of 2 M HCl, and extracted with 50 mL of chloroform three times. The combined chloroform layer was dried over sodium sulfate anhydrous, and the solvents were evaporated *in vacuo*. **5** was obtained as a yellow powder (0.28 g, 0.58 mmol) in 80% yield. M.p. 118.5–119.7 °C; ^1H NMR (400 MHz, $CDCl_3$) $\delta = 0.88$ (t, $J = 6.9$ Hz, 3H, $PhO(CH_2)_{13}\mathit{CH_3}$), 1.22–1.52 (m, 22H, $PhOCH_2CH_2(\mathit{CH_2})_{11}$), 1.82 (tt, $J = 6.9$, 6.2 Hz, 2H, $PhOCH_2\mathit{CH_2}$), 2.01 (tt, $J = 7.6$, 7.4 Hz, 2H, $PhCH_2\mathit{CH_2}$), 2.41 (t, $J = 7.4$ Hz, 2H, $Ph\mathit{CH_2}$), 2.75 (t, $J = 7.6$ Hz, 2H, $PhCH_2CH_2\mathit{CH_2}$), 4.03 (t, $J = 6.6$ Hz, 2H, $PhO\mathit{CH_2}$), 6.99 (d, $J = 9.0$ Hz, 2H, 2, 6-H Ar), 7.31 (d, $J = 8.5$ Hz, 2H, 3′, 5′-H Ar), 7.81 (d, $J = 8.5$ Hz, 2H, 2′, 6′-H Ar), 7.89 ppm (d, $J = 9.0$ Hz, 2H, 3, 5-H Ar).

Triphenylene-2,3,6,7,10,11-hexayl hexakis[4-(4-{[4-(tetradecyloxy)phenyl]diazenyl}phenyl)butanoate] (1-C14). 0.266 g (0.55 mmol) of **5** and 0.48 mL (0.55 mmol) of oxalic dichloride were poured into 45 mL of toluene anhydrous, and the mixture was refluxed for 2 h to form acid chloride **6**, and the toluene solvent was removed by distillation (stopping cooling water of the condenser) to remove the formed oxalic acid and excess oxalic dichloride. Then 50 mL of fresh toluene anhydrous was added to the mixture and stirred for another 2 h, and the solution was concentrated to 20 mL by evaporation of the solvent in the same manner. In another flask, 0.03 g (0.09 mmol) of purified 2,3,6,7,10,11-hexahydroxytriphenylene and 0.05 mL (0.67 mmol) of pyridine was dissolved into 700 mL of dichloromethane anhydrous, and added the 20 mL of toluene solution of acid chloride followed by refluxing for three days. After the reaction was complete, solvents were removed and the product was purified by silica gel chromatography (chloroform anhydrous) followed by recrystallization from chloroform anhydrous to obtain 0.040 g (0.013 mmol) of **1-C14** as a yellow powder in 14.4% yield. M.p. 206.3–207.1 °C; ^1H NMR (400 MHz, $CDCl_3$) $\delta = 0.88$ (t, $J = 6.9$ Hz, 18H, $PhO(CH_2)_{13}\ \mathit{CH_3}$), 1.20–1.60 (m, 132H, $PhOCH_2CH_2(\mathit{CH_2})_{11}$), 1.80 (tt, $J = 7.0$, 6.6 Hz, 12H, $PhOCH_2\mathit{CH_2}$), 2.11 (tt, $J = 7.6$, 7.5 Hz, 12H, $PhCH_2\mathit{CH_2}$), 2.62 (t, $J = 7.5$ Hz, 12H, $PhCH_2CH_2\mathit{CH_2}$), 2.78 (t, $J = 7.6$ Hz, 12H, $Ph\mathit{CH_2}$), 4.01 (t, $J = 6.6$ Hz, 12H, $PhO\mathit{CH_2}$), 6.97 (d, $J = 9.0$ Hz, 12H, azobenzene2, 6-H Ar), 7.31 (d, $J = 8.3$ Hz, 12H, azobenzene3′, 5′-H Ar), 7.81 (d, $J = 8.3$ Hz, 12H, azobenzene2′, 6′-H Ar), 7.87 (d, $J = 9.0$ Hz, 12H, azobenzene3, 5-H Ar), 8.24 ppm (s, 6H, triphenylene1,4,5,8,9,12-H Ar); IR (C=O): 1754 cm^{-1}. Anal. calcd for $C_{198}H_{264}N_{12}O_{18}$: C 76.71, H 8.58, N 5.42; found: C 76.72, H 8.60, N 5.42%.

Apparatus

DSC measurements were carried out on TA Instruments, DSC2920 and Perkin Elmer DSC 8500, and the curve fitting by Gauss function was applied. Optical microscopy was performed using an OLYMPUS, BH2 equipped with an LINCAM MK600 hot stage and a Leica DMLP equipped with an LINCAM MK600 hot stage or METLLER FP82HT hot stage. For the protection of UV and visible light ($\lambda < 580$ nm) under observation of an optical microscope, a cut filter (TOSHIBA Color Filter O-58) was used. For the UV irradiation to photoreaction of azobenzene moieties under optical microscopic observation, a UV-LED (KEYENCE, UV-400) attached with a UV-50H (365 nm) was applied. For the isomerisation of the derivative in solution, an UV hand lamp (TOPCON, Fi-5L, 365 nm) was used. Absorption spectra were measured on HITACHI, U-3500, and OTSUKA ELECTRONICS, MCPD-2000 spectrophotometers, and XRD was measured on an X-ray diffractometer (RIGAKU, RINT2000).

Observations of LC phases (mesomorphism). DSC measurements were carried out with TA Instruments, DSC2920 Modulated DSC. The optical texture observation was performed with a polarised microscope (Olympus BH2) equipped with a temperature-controlled hot stage (Mettler FP82HT and FP90). X-Ray diffraction measurements were carried out with a RIGAKU RINT2000 X-ray diffractometer, and the temperature of a sample was controlled on a hand-made hot stage.

Photo-induced phase transitions. Absorption spectra were measured with an absorption spectrophotometer (Hitachi U-3410). Visible light was irradiated by using a 500 W Xe-arc lamp (USHIO SX-Ul501XQ). A UV-LED (UV-400, KEYENCE) with a UV-50H attachment ($\lambda = 365$ nm) was used as the UV light source for the photo-orientation of liquid crystal phase transitions. LC phase transitions were monitored using a Leica polarised microscope equipped with a Shimadzu Moticam 2000 video recording system and a LINKAM MK600 hot stage.

Acknowledgements

We would like to thank Prof. Shusaku Nagano and Prof. Takahiro Seki for their help in the absorption spectral measurements at high temperatures and thermal imaging photography. We also thank Prof. Hiroshi Miyasaka and Dr Tetsuro Katayama for the flash photolysis of the liquid crystal at 200 °C. K.U. thanks S. Yokojima for his helpful discussions.

Notes and references

1 *Handbook of Liquid Crystals: Fundamentals*, ed. D. Demus, J. Goodby, G. W. Gray, H. W. Spiess and V. Vill, Wiley-VCH, 1998.
2 B. M. Rosen, C. J. Wilson, D. A. Wilson, M. Peterca, M. R. Imam and V. Percec, *Chem. Rev.*, 2009, **109**, 6275.
3 B. Donnio, S. Buathong, I. Bury and D. Guillon, *Chem. Soc. Rev.*, 2007, **36**, 1495.
4 Y. Shimizu, A. Kurobe, H. Monobe, N. Terasawa, K. Kiyohara and K. Uchida, *Chem. Commun.*, 2003, 1676.
5 S. Silong, L. Rahman, W. W. M. Z. Yunus, M. Z. Rahman, M. Ahmad and J. Haron, *Mater. Res. Soc. Symp. Proc.*, 2002, **709**, 105.
6 K. Ichimura, *Chem. Rev.*, 2000, **100**, 1847.
7 (*a*) T. Ikeda and O. Tsutsumi, *Science*, 1995, **268**, 1873; (*b*) T. Ikeda, *J. Mater. Chem.*, 2003, **13**, 2037.
8 R. Hori, D. Furukawa, K. Yamamoto and S. Kutsumizu, *Chem.–Eur. J.*, 2012, **18**, 7346.
9 S. Furumi, M. Kidowaki, M. Ogawa, Y. Nishiura and K. Ichimura, *J. Phys. Chem. B*, 2005, **109**, 9245.
10 *Photochromism Molecules and Systems*, ed. H. Duerr and H. Bouas-Laurent, Elsevier, Amsterdam, The Netherlands, 1990.
11 H. Rau, *Angew. Chem., Int. Ed. Engl.*, 1973, **12**, 224.
12 D. Aronzon, E. P. Levy, P. J. Collings, A. Chanishvili, G. Chilaya and D. Petriashvili, *Liq. Cryst.*, 2007, **34**, 707.
13 S. Yagai, T. Nakajima, K. Kishikawa, S. Kohmoto, T. Karatsu and A. Kitamura, *J. Am. Chem. Soc.*, 2005, **127**, 11134.
14 (*a*) M. O'Niell and S. M. Kelly, *Adv. Mater.*, 2011, **23**, 566; (*b*) W. Pisula, M. Zorn, J. Y. Chang, K. Müllen and R. Zentel, *Macromol. Rapid Commun.*, 2009, **30**, 1179; (*c*) M. Funahashi, *Polym. J.*, 2009, **41**, 459; (*d*) S. Sergeyev, W. Pisula and Y. H. Geerts, *Chem. Soc. Rev.*, 2007, **36**, 1902; (*e*) S. Laschat, A. Baro, N. Steinke, F. Giesselmann, C. Hägele, G. Scalia, R. Judele, E. Kapatsina, S. Sauer, A. Schreivogel and M. Tosoni, *Angew. Chem., Int. Ed.*, 2007, **46**, 4832; (*f*) Y. Shimizu, K. Oikawa, K. Nakayama and D. Guillon, *J. Mater. Chem.*, 2007, **17**, 4223.
15 F. Ilievski, A. D. Mazzeo, R. F. Shepherd, X. Chen and G. M. Whitesides, *Angew. Chem., Int. Ed.*, 2011, **50**, 1890.